LASER CALIBRATION OF THE ATLAS TILE CALORIMETER

Giulia Di Gregorio – INFN-Pisa, on behalf of the ATLAS Tile Calorimeter System

High performance stability of the ATLAS Tile calorimeter is achieved with a set of calibration procedures. One step of the calibration procedure is based on measurements of the response stability to laser excitation of the PMTs that are used to readout the calorimeter cells. A facility to study in lab the PMT stability response is operating in the PISA-INFN laboratories since 2015. Goals of the tests in lab are to study the time evolution of the PMT response to reproduce and to understand the origin of the response drifts seen with the PMT mounted on the Tile calorimeter in its normal operating during LHC run I and run II.
A new statistical approach was developed to measure the drift of the absolute gain. This approach was applied to both the ATLAS laser calibration data and to the data collected in the Pisa local laboratory. The preliminary results from these two studies are shown.

ATLAS Tile Calorimeter (TileCal)

The Tile Calorimeter (TileCal) is central section of the hadronic calorimeter in the ATLAS detector, having major importance for measuring hadrons, jets, taus and missing transverse energy.

It is a sampling calorimeter made up of steel and scintillating tiles. Tiles are coupled to optical fibers and read-out by photomultiplier tubes (PMT). The grouping of fibers defines the unit cell: a typical cell is composed of two channels corresponding to the two PMTs.

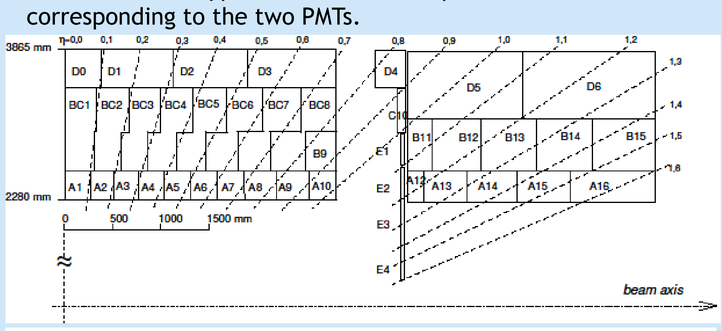

Fig. 2: TileCal cell map denoted by a letter (A to E) plus a number.

TileCal response is calibrated via three systems (Cesium source, laser light, charge injection) in order to monitor independently the different parts of the readout chain. Additionally Minimum Bias events ("particles" in Fig. 3) are used to provide an independent cross-check of Cs calibration. The laser system monitors both the PMTs and the front-end electronics used for data acquisition. Light pulses similar to those produced by ionizing particles are transmitted simultaneously at all TileCal PMTs through a bundle of about 100 meter long clear fiber.

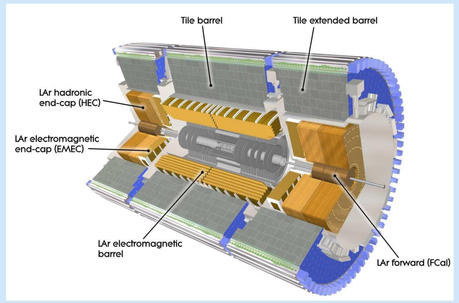

Fig. 1: ATLAS inner detector and calorimeters.

A continuous percent-level calibration of each cell is required to maintain the calorimeter high performance. PMT response stability to fixed intensity light signal is required. Drift of the global PMT response are measured with the Tile calibration system and calibration constants are applied to the raw data from individual detector channel.

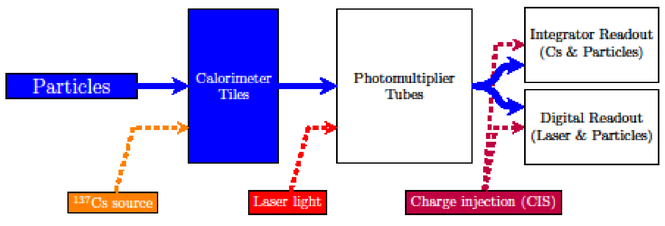

Fig. 3: Scheme of TileCal calibration chain.

The laser II system

The laser system has been upgraded for 2015 LHC run, with the goal to achieve laser monitor stability at the sub-percent level, including :

- ✓ A re-design of the optical and the mechanical system distributing laser light to improve its stability.
- ✓ New internal calibration scheme to cope with the increase of the number of photodiodes used to monitor the laser light.
- ✓ Innovative electronics to drive the system, perform signal digitization, and communicate with ATLAS DAQ

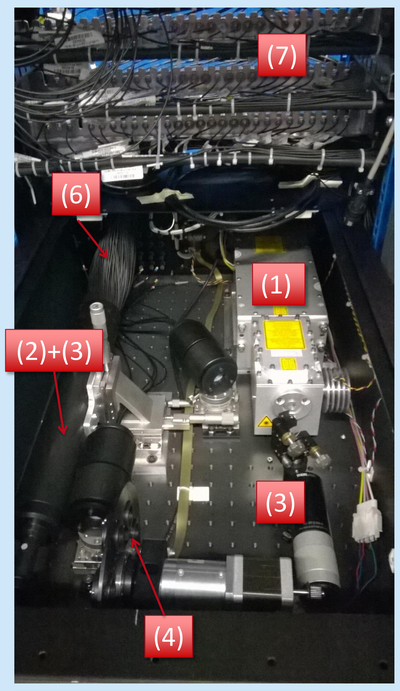

Fig. 5: Final setup of the optics box.

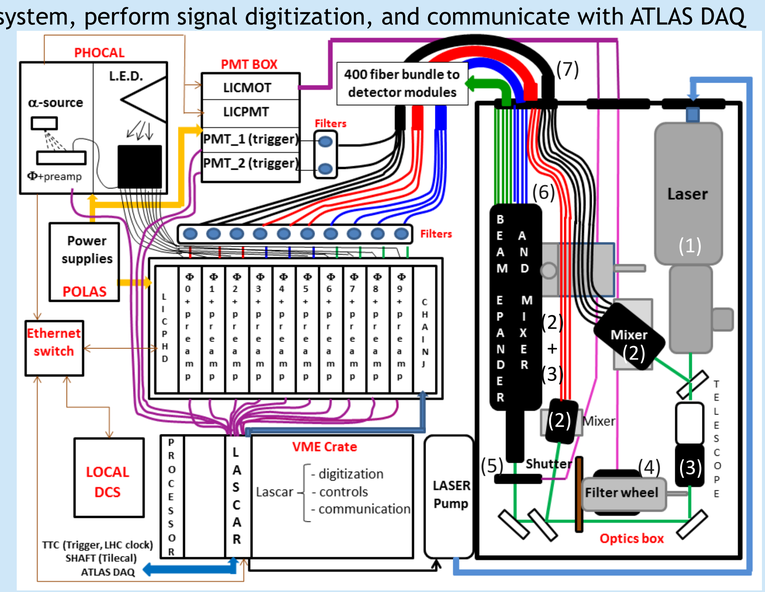

Fig. 4: Scheme of the upgraded laser system.

——— : laser light path from laser head to the detector

DETAILS OF LASER OPTIC BOX

(1): laser; (2): mixer; (3): beam-expander; (4): filter wheel; (5): shutter; (6): bundle of clear fibers bringhing laser light to the detector and the monitors; (7): fiber patch panel;

Pisa experimental setup

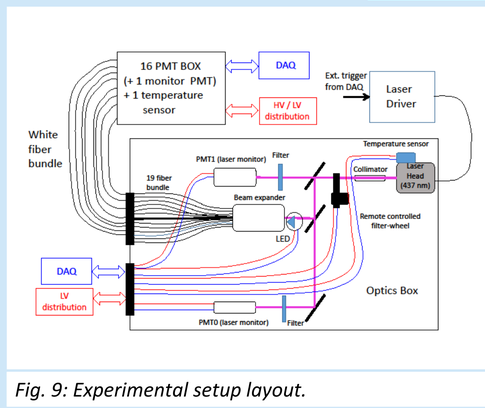

Fig. 9: Experimental setup layout.

A local test bench for PMT robustness is operating in the Pisa-INFN labs. The optical system to excite the tested PMTs (Fig. 9) is similar to the one used fot the laser calibrations of Tile PMTs (Fig. 5). The test bench set-up is characterized by:

- ✓ Light sources (alternate operation):
  1. A 437 nm laser, 80 ps pulses width;
  2. A 532 nm LED, 150 ns pulses width;
- ✓ Laser beam intensity is varied with a remote controlled filter wheel and monitored with two PMTs;
- ✓ Laser pulses are used to measure the response of the PMTs under test;
- ✓ The monitor PMT signals are used for normalization purposes;
- ✓ LED pulses are used to excite and to integrate large amounts of anode charge for the PMTs under test in the PMT box;
- ✓ The light from the sources is expanded and fed to the PMT box through a white fiber bundle;
- ✓ All PMT signals are digitized with charge integration ADCs.

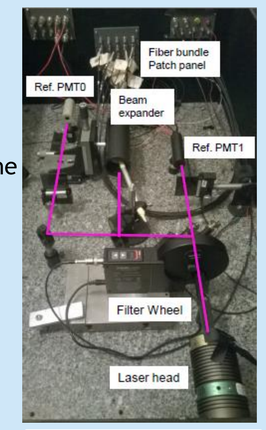

Fig. 10: Pisa optic box

The statistical method for measuring the PMT absolute gain

- ✓ Assume pure Poisson statistics for the photo-electron extraction and multiplication;
- ✓ Assume spatial and temporal coherence for the laser source;
- ✓ All electronic noise contributions to the signal fluctuations can be neglected;
- ✓ Only the photostatistics and the laser intensity fluctuations contribute to the signal variance:

$$\frac{Var(q)}{< q >^2} = f \cdot \left(\frac{\sigma_N^2}{< N >^2} + \frac{Var(I)}{< I >^2} \right) \qquad (1)$$

<q> is the average anode charge; <N> is the average number of photon electron;
<I> is the average light intensity of a pulsed source on the cathode; f is the noise excess factor

If G is the PMT gain at a given voltage : $< q > = N \cdot G \cdot e$ (e is the electron charge). In the Poisson statistics $\sigma_N^2 = < N >$ so substituting in equation (1):

$$\frac{Var(q)}{< q >} = f \cdot G \cdot e + f \cdot k \cdot < q > \qquad (2)$$

where $k = \frac{Var(I)}{<I>^2}$ is the coherence factor.

Pisa measurements

The factor k can be statistically evaluated with two methods:

$$k = \frac{\frac{Var(q_n)}{q_n} - \frac{Var(q_m)}{q_m}}{<q_n> - <q_m>} \qquad (3)$$

here n and m is referred to the same PMT response at two different light intensity.

Alternatively:

$$k = \frac{Cov(q_i, q_j)}{< q_i >< q_j >} \qquad (4)$$

here q_i and q_j are the anode charges of any PMT pairs receiving similar fractions of the same light pulses at fixed intensity.

Fig. 11 shows the evolution of the PMT gain of 4 tested samples. The gain is calculated with:

1. the intensity scan method (open circles) (equation (3))
2. covariance method (full circles) (equation (4))

On day 20/01/2017 the PMT HV was increase from 700V to 830V.

The expected increase of the gain by a factor of about 1.5-2.5 is measured in all cases.

The covariance method appears to be more precise, but a very general agreement between the two methods is observed.

Measurements done with never used PMTs, model Hamamatsu R11187, an evolution of R7877 mounted on Tile.

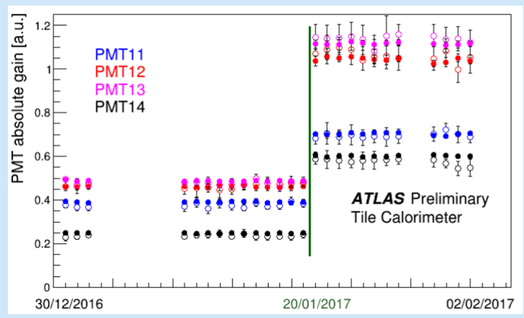

Fig. 11: PMT gain at different HV values.

Time stability of the PMT response at ATLAS

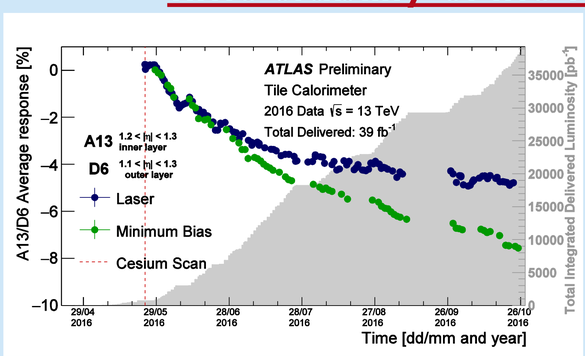

Fig. 6: Evolution of A13/D6 response to laser pulses (blue) and minimum bias (green). Grey area: integrated luminosiity.

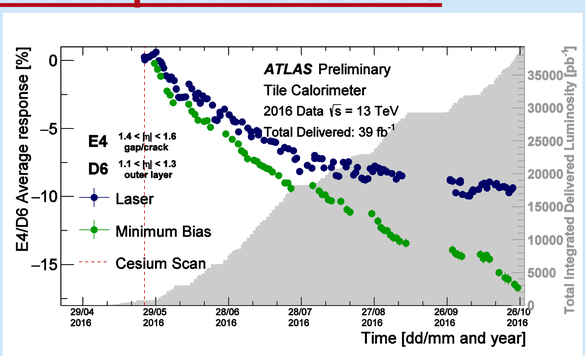

Fig. 7: Evolution of E4/D6 response to laser pulses (blue) and minimum bias (green). Grey area: integrated luminosity

In Fig. 6 and 7 average variation of the A13 and E4 cells in the observation period is shown for their response to laser calibration and to Minimum Bias (MB) events. The observation period begins on May 24th 2016, last detector global calibration with Cesium source system (vertical red dashed line in Fig. 6 and 7) and it ends on October 27th. The variations observed by MB are sensitive to PMT drift and scintillator irradiaton.

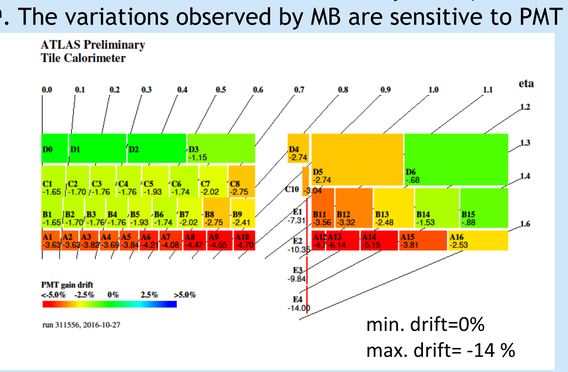

min. drift=0%
max. drift= -14 %

Fig. 8: TileCal cell map with PMTs drifts.

The average down-drift of each cell type in the observation period is shown in the map in Fig. 8. The drift of each PMT is measured using laser calibration system that sends a controlled amount of light in the photocathode of each PMT in the absence of collisions. For each cell, the PMT variation is defined as the mean of the Gaussian function that fits the PMT variation distribution of the channels associated to this cell.

The observed down-drift mostly affects cells in the inner radius that are the cells with higher exposure.

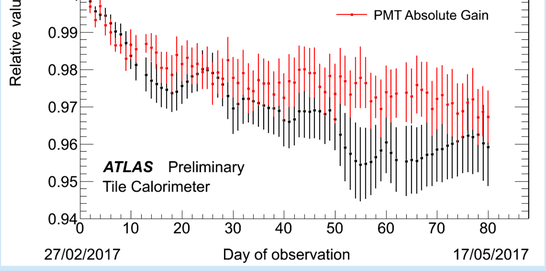

Fig. 12: PMT response and PMT absolute gain evolution.

The picture shows the time evolution of the PMT response (black) and PMT absolute gain (red) normalized to the first day of observation and to the signal of a reference PMT monitoring the light source intensity. Each point is the average over the response of 9 PMTs dismounted from TileCal detector in February 2017 (model Hamamatsu R7877). They were reading out different cell type (A, BC, D, E) having integrated 1 to 5 C during run-I and run-II. The average integrated charge during the test bench operation is 20 C so the typical down-drift per integrated charge is about -0.2%/C. The average down-drift of the PMT response per unit of integrated charged measured at the test bench is compatible with the corresponding down-drift observed for the response of the PMTs installed on detector.

Estimate PMT response loss at HL-LHC era

Time evolution of the PMT response shows a fairly exponential decay shape both for measurements of on-detector sample (Fig. 6-7) and for test bench measurements (Fig. 12). Assuming an exponential decay of the PMT response as a function of the integrated charge, we fit with an exponential function the average response evolution of same type cells in the detector. We extract the decay constant for each cell type from their response evolution during LHC run I (20 fb^{-1} integrated luminosity) and run II (35 fb^{-1} integrated luminosity in 2015/2016). We use the measured decay constants to make projections to larger amount of integrated charge (i.e. Integrated luminosity) as expected for HL-LHC era as shown in table 13. At the end of HL-LHC era, most exposed PMTs (A13 cells) are expected to loose 50 % of their response.

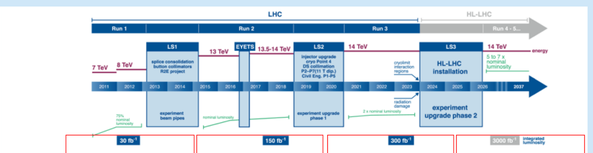

Most exposed cell per layer	PMT integrated anode charge (C)	Measured PMT response loss (%)	PMT integrated anode charge (C)	Measured PMT response loss (%)	PMT integrated anode charge (C)	Measured PMT response loss (%)	PMT integrated anode charge (C)	Measured PMT response loss (%)
	30 fb^{-1}		150 fb^{-1}		300 fb^{-1}		3000 fb^{-1}	
A13	5	-5	25	-15	50	-20	500	-50
B11/C10	1.5	>-3	8	-5	15	-7	150	-15
D4	1	>-2	5	-2.5	10	-6	100	-9

Fig. 13: Predicted PMT response loss.